THE JOURNAL OF PHYSICAL CHEMISTRY Letters

pubs.acs.org/JPCL Letter

New Insights into the Charge-Transfer-to-Solvent Spectrum of Aqueous Iodide: Surface versus Bulk

Dhritiman Bhattacharyya,[‖] Hikaru Mizuno,[‖] Anthony M. Rizzuto, Yuyuan Zhang, Richard J. Saykally,* and Stephen E. Bradforth*

Cite This: J. Phys. Chem. Lett. 2020, 11, 1656−1661 Read Online

ACCESS | Metrics & More | Article Recommendations | Supporting Information

ABSTRACT: Liquid phase charge-transfer-to-solvent (CTTS) transitions are important, as they serve as photochemical routes to solvated electrons. In this work, broadband deep-ultraviolet electronic sum frequency generation (DUV-ESFG) and two-photon absorption (2PA) spectroscopic techniques were used to assign and compare the nature of the aqueous iodide CTTS excitations at the air/water interface and in bulk solution. In the one-photon absorption (1PA) spectrum, excitation to the 6s Rydberg-like orbital (5p → 6s) gives rise to a pair of spin−orbit split iodine states, $^2P_{3/2}$ and $^2P_{1/2}$. In the 2PA spectra, the lower-energy $^2P_{3/2}$ peak is absent and the observed 2PA peak, which is ∼0.14 eV blue-shifted relative to the upper $^2P_{1/2}$ CTTS peak seen in 1PA, arises from 5p → 6p electronic promotion. The band observed in the ESFG spectrum is attributed to mixing of excited states involving 5p → 6p and 5p → 6s promotions caused by both vibronic coupling and the external electric field generated by asymmetric interfacial solvation.

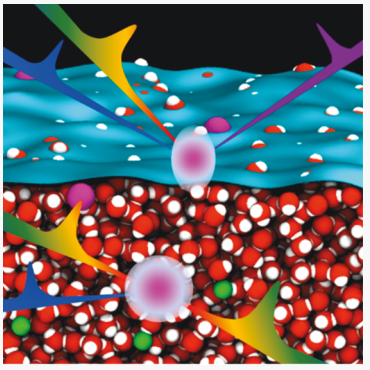

In investigating the behavior of halides, pseudohalides, and biologically relevant anions in aqueous systems, many studies[1−7] have focused on charge-transfer-to-solvent (CTTS) transitions, the precursors of solvated electrons. CTTS states are short-lived excited states that comprise a neutral parent atom and an excited electron in a dipole-bound state supported by the surrounding solvent network. Because the initial and final states are defined by the parent ion and the surrounding solvent, CTTS spectra are highly sensitive to the environment, e.g., solvation, temperature, pressure, and electrolytes.[1,5,8,9] Excitation to a CTTS state can lead to the formation of solvated electrons with a high quantum yield;[10,11] the high sensitivity to the local environment and large extinction coefficients of CTTS transitions make them excellent probes of anion solvation dynamics in complex systems.

Iodide has served as a prototype of local solvation structure due to its favorable spectroscopic properties. The lowest-energy CTTS bands of iodide in the deep ultraviolet (UV) (∼190−260 nm) are easily accessible experimentally, as compared to those of lighter halides that exhibit CTTS bands at higher energies. Furthermore, iodide is a spherical, monatomic anion with only electronic degrees of freedom, thus making theoretical calculations and modeling more straightforward than for polyatomic ions, which become further complicated by the presence of overlapping intramolecular valence excitations and orientational effects. At room temperature, the bulk one-photon absorption (1PA) spectrum of the aqueous iodide CTTS band exhibits well-resolved doublet components at 226 nm (5.5 eV) and 193 nm (6.4 eV) with similar intensities (Figure 1a).[12] Because the doublet splitting roughly matches the energy difference (0.9 eV) between the ground state ($^2P_{3/2}$) and spin-orbit excited state ($^2P_{1/2}$) of the neutral iodine atom, they are commonly termed the $J = {}^3/_2$ and $J = {}^1/_2$ bands, respectively. Previously, the 1PA spectrum has been fit with sets of overlapping log-normal bands derived from spectra in various solvents and conditions, suggesting that the iodide CTTS spectrum consists of several additional overlapping transitions at higher energies,[13−15] as shown in Figure S1. The higher-energy bands have not yet been assigned definitively but are thought to arise from higher-lying CTTS excited states.[13,14] In this work, we focus on elucidating the nature of the transitions that make up these CTTS bands.

Resonant one-photon excitation into the lower-energy $J = {}^3/_2$ CTTS band detaches an electron on a 200 fs time scale, which, in turn, relaxes in ∼800 fs,[16,17] consistent with theoretical results of Sheu and Rossky.[18,19] Upon resonant one-photon excitation into the higher-lying CTTS state ($J = {}^1/_2$), an additional autodetachment channel for hydrated electron formation is proposed,[20] which is characterized by an ejection length that is different from that of the lower $J = {}^3/_2$ pathway.[21,22] Phase-sensitive transient second harmonic generation spectroscopy measurements by Verlet and co-workers reveal that the lowest CTTS state of aqueous iodide at the air/water interface is asymmetrically solvated in the plane

Received: December 26, 2019
Accepted: February 10, 2020
Published: February 10, 2020

https://dx.doi.org/10.1021/acs.jpclett.9b03857
J. Phys. Chem. Lett. 2020, 11, 1656−1661

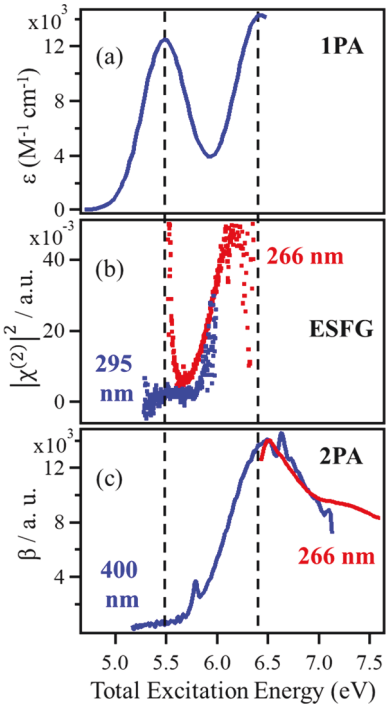

Figure 1. Charge-transfer-to-solvent spectra of aqueous iodide. (a) 1PA spectrum of potassium iodide in water at 298 K. The literature deconvolution of the overall absorption spectrum into individual CTTS bands is shown in Figure S1. The vertical dashed lines correspond to the 1PA peak positions for the two lowest CTTS transitions at 298 K and 1 atm for aqueous NaI. (b) Normalized ESFG spectra of aqueous NaI for two different pump wavelengths (ω_1 = 266 and 295 nm; $\omega_2 \approx$ 600−1400 nm; $[NaI]_{bulk}$ = 5 M) measured at 293 K. For the 266 nm pump, the ESFG intensity is truncated in the lower-energy region. (c) 2PA spectra of aqueous NaI for two different pump wavelengths (ω_1 = 266 and 400 nm; $\omega_2 \approx$ 310−700 nm; $[NaI]_{bulk}$ = 700 mM) measured at 293 K. The sharp features in the 400 nm spectra are due to the instantaneous Raman signals from water.

of the surface and that the electron solvation dynamics at the interface are very similar to those observed in the bulk, although slightly faster.[23,24] The asymmetry of the lowest CTTS wave function is also predicted by Bradforth and Jungwirth,[21] arising from the thermal fluctuation of the local solvation environment. Their calculation suggests that the lowest CTTS states comprise a mixture of valence s (∼30%), diffuse s (∼50%), and p (∼17%) type orbitals. This result contrasts with the calculation by Sheu and Rossky that predicted ∼45−80% d orbital character in the lowest CTTS states.[25] This discrepancy most likely arises from the one-electron model used by Sheu and Rossky that did not include all of the valence shell electrons of iodide,[25] resulting in artificial lowering of the virtual d orbitals. The Configuration Interaction Singles (CIS) calculation by Bradforth and Jungwirth[21] in fact predicted promotions involving orbitals with considerable d character are situated much higher in energy, as compared to the lowest CTTS states. Although the lowest-energy CTTS transition has been studied extensively using linear absorption spectroscopy, very little is known about the character of the higher-lying CTTS states of aqueous iodide because of their overlapping nature and the onset of the lowest-lying water electronic absorption (∼6.4 eV). The latter increasingly interferes with the shorter wavelength region of the 1PA spectra.[9] Herein, we present aqueous iodide CTTS spectra measured with interface-sensitive femtosecond broadband deep-UV electronic sum frequency generation (DUV-ESFG) spectroscopy and bulk-sensitive two-photon absorption (2PA) spectroscopy and discuss the salient selection rules and symmetry arguments within a Rydberg transition model to provide insight into the aqueous iodide CTTS spectrum, specifically in the region of overlapping transitions. Moreover, the interference from water electronic absorption is avoided by virtue of using nonlinear processes to access the halide electronic absorption. None of the input photon energies overlaps with the onset of water electronic absorption, and as shown previously,[26] the 2PA threshold for bulk water absorption lies even higher in energy (∼7.8 eV), indicating that water is two-photon transparent in the energy region explored in this work.

Second-order nonlinear optical spectroscopy, which includes second harmonic generation (SHG) and sum frequency generation (SFG), has often been used to study interfaces due to its inherent surface specificity. Under the electric dipole approximation, the second-order nonlinear susceptibility $[\chi^{(2)}]$ vanishes in centrosymmetric media, and SHG and SFG spectroscopies are surface-sensitive probes of the air/water interface with a probe depth of ∼1 nm, corresponding to a few outermost monolayers.[27−29] In both cases, the measured output signal can be resonantly enhanced when the frequency of either or both input photons and/or the sum frequency photon matches a dipole-allowed transition in the molecule, atom, or ion at the interface. The selection rules for electronic SFG and SHG spectroscopy wherein the transition is resonant exclusively at the sum frequency require the transition to be simultaneously active in both 1PA and 2PA (eq 1).[30,31]

$$I \propto |\chi^{(2)}|^2 \propto \sum_n \frac{|\mu_{0n}(\alpha_{0n})_{2PA}|^2}{(\omega_{CTTS} - \omega_1 - \omega_2)^2 + \Gamma_{CTTS}^2} \quad (1)$$

where $\chi^{(2)}$ is the second-order nonlinear susceptibility, μ_{0n} is the 1PA transition dipole matrix element, $(\alpha_{0n})_{2PA}$ is the 2PA polarizability tensor element connecting the ground state to excited state n, Γ_{CTTS} is the line width of the CTTS transition, ω_{CTTS} is the transition energy between the ground state and CTTS excited state, and ω_1 and ω_2 are the frequencies of the input radiations.

Pointwise interfacial $|\chi^{(2)}|^2$ spectra of iodide were measured with resonant deep-UV electronic SHG spectroscopy developed by the Saykally group in the 2000s.[32] By fitting to a Langmuir adsorption model, Petersen et al. obtained Gibbs free energies of adsorption (ΔG_{ads}) for iodide at the air/water interface of −6.1 ± 0.2 and −6.3 ± 0.2 kcal/mol for NaI and KI salts, respectively.[33] However, noisy, time-consuming, and error-prone pointwise ESHG spectra present a challenge for quantitative analysis of spectral shapes and shifts.

To measure broadband electronic spectra at the air/water interface, femtosecond broadband DUV-ESFG spectroscopy was recently developed by the Saykally group.[34,35] The detailed experimental scheme is described elsewhere.[34,35] Briefly, a narrowband, 100 fs tunable UV pulse (ω_1) is spatially and temporally overlapped with a white light continuum pulse (WLC, ω_2) at the solution surface, generating coherent sum frequency ($\omega_1 + \omega_2$) photons at the phase-matched angle in reflection geometry. The continuum pulse enables the acquisition of a broadband spectrum in a single measurement without having to tune the input frequencies. We previously

https://dx.doi.org/10.1021/acs.jpclett.9b03857
J. Phys. Chem. Lett. 2020, 11, 1656−1661

reported the CTTS spectrum of iodide ($[NaI]_{bulk}$ = 5 M) at the air/water interface measured by this broadband DUV-ESFG approach with an ω_1 of 266 nm and an ω_2 of ≈600−1400 nm. The interfacial $|\chi^{(2)}|^2$ spectrum (Figure 1b, red) appeared to reveal a small red-shift of the CTTS doublet, a slight narrowing of the line widths, and a large relative intensity difference between the upper ($J = {}^1/_2$) and lower ($J = {}^3/_2$) CTTS bands compared to the bulk 1PA spectrum.[34] To clearly show the $J = {}^1/_2$ CTTS transition, the 266 nm ESFG spectrum is truncated in the region of the intense band at a lower energy ($J = {}^3/_2$). In the work presented here, we supplement this $|\chi^{(2)}|^2$ spectrum with data measured with an ω_1 of 295 nm.

The interfacial $|\chi^{(2)}|^2$ spectrum (ω_1 = 295 nm, and ω_2 ≈ 600−1400 nm) exhibits no significant resonance enhancement for the lower ($J = {}^3/_2$) CTTS band under the strictly two-photon resonance condition (Figure 1b, blue). We attribute the large relative intensity difference observed in the previously reported spectrum (ω_1 = 266 nm) to a double resonance effect of the $J = {}^3/_2$ band, wherein the narrowband 266 nm pulse is also one-photon resonant with the tail of the lower-energy $J = {}^3/_2$ band, leading to an additional resonance enhancement term in the denominator (eq 2).[30,31]

$$I_{ESFG} \propto |\chi^{(2)}|^2 \propto \sum_n \frac{|\mu_{0n}(\alpha_{0n})_{2PA}|^2}{[(\omega_{CTTS} - \omega_1 - \omega_2)^2 + \Gamma_{CTTS}{}^2][(\omega_{CTTS} - \omega_1)^2 + \Gamma_{CTTS}{}^2]} \quad (2)$$

This is consistent with the fact that aqueous iodide has been used as a precursor of solvated electrons by employing a 266 nm laser to excite the lower-energy CTTS band.[36,37] The fact that the $J = {}^3/_2$ CTTS band of iodide has no ESFG intensity under the strictly two-photon resonant condition (ω_1 = 295 nm) suggests that the transition must be two-photon inactive.

To verify this hypothesis, broadband 2PA spectra of a 700 mM bulk aqueous NaI solution were measured, as shown in Figure 1c. Interestingly, continuous two-photon absorption spectra have not been reported before for any aqueous alkali halide salt. Two different pump wavelengths (266 and 400 nm) along with the visible portion of the white light continuum (310−700 nm) were used to cover the spectral range of the iodide CTTS doublet. Both pump and probe beams were overlapped spatially and temporally on a wire-guided gravity jet.[38] The differential absorbance ($A_{pump\text{-}on} - A_{pump\text{-}off}$) of the broadband continuum probe was recorded with and without the pump pulse using a 256-channel silicon photodiode array. The detailed experimental design employed is described elsewhere.[26,39] Although the 1PA spectrum shows similar intensities for the $J = {}^3/_2$ and $J = {}^1/_2$ bands, the former is absent in the 2PA spectrum, consistent with the broadband ESFG surface spectra presented above. The nature of the orbital excitations resulting in the CTTS transitions in aqueous iodide and the reasons for the absence of the lowest CTTS band in 2PA will be discussed below.

Several studies dating back to a classic paper by Franck and Scheibe[40] suggest that the promoted electron in the vertical excited state of aqueous iodide is spatially extended over the solvent shell but still centered on the parent iodine atom.[41,42] Hence, in the simple Rydberg transition model,[43] the excited electronic configuration is $[Kr]4d^{10}5s^25p^56s^1$, which gives rise to four excited states ($^3P_2$, $^3P_1$, $^3P_0$, and $^1P_1$) in the Russell-Saunders (R-S) coupling limit (Figure 2). However, for a heavy atom like iodine, the significance of the R-S term

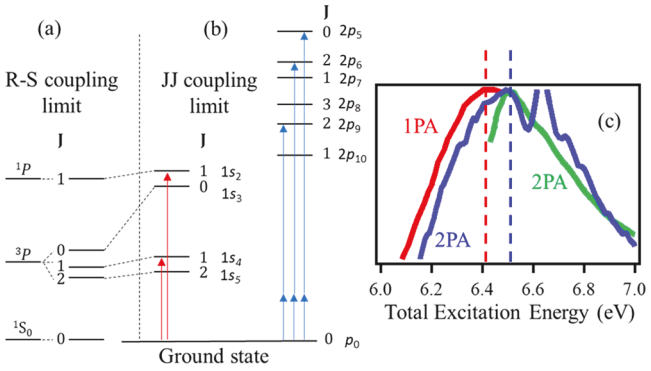

Figure 2. Energy levels of xenon (isoelectronic with I^-) and transitions from ground to excited states.[47] Two different coupling schemes are shown: (a) R−S coupling and (b) J−J coupling. The Paschen notations, as shown in Table 1, are used to designate the energy levels. The red and blue arrows are used to show the 1PA and 2PA excitations, respectively. (c) Close-ups of the 1PA and 2PA spectra of aqueous iodide in the region of the higher-energy CTTS transition clearly showing the shift in the peak position. The 1PA spectrum is reproduced from ref 9 measured at 298 K and 250 bar.

symbols is obscured because the orbital angular momentum (L) and spin angular momentum (S) are no longer good quantum numbers. Instead, the *jj* coupling language is more relevant and the total angular momentum ($J = L + S$) should be used to more accurately describe the atomic energy levels.[44]

In the *jj* coupling limit, the selection rule for 1PA requires $\Delta J = 0, \pm 1$ with the restriction that the transition between the $J = 0$ and $J = 0$ states not be allowed, and for 2PA, $\Delta J = 0, \pm 1, \pm 2$ holds. From the $J = 0$ ground state of the iodide anion, 1PA transitions to both upper and lower spin-orbit split components are allowed (Figure 2b, red arrows).[44] The selection rules further dictate that both of these transitions would also be allowed in 2PA, which fails to explain our experimental findings. However, it is also important to consider the parity of the states involved in the electronic transitions. We resort to the spectroscopic database compiled by Moore,[45] wherein the excited state energies and their corresponding term symbol notations for xenon are tabulated (Table 1). Because I^- is isoelectronic with Xe, the energy ordering of the excited states and the corresponding term

Table 1. Electronic Excited States of Xenon as Adapted from the Database Compiled by Moore[45]

Paschen notation	configuration	designation		J	energy (eV)
p_0	$5p^6$	$5p^6$	^1S	0	0.00
$1s_5$	$5p^5(^2P^\circ_{3/2})6s$	6s	[3/2]°	2	8.32
$1s_4$				1	8.44
$1s_3$	$5p^5(^2P^\circ_{1/2})6s$	6s′	[1/2]°	0	9.45
$1s_2$				1	9.57
$2p_{10}$	$5p^5(^2P^\circ_{3/2})6p$	6p	[1/2]	1	9.58
$2p_9$	$5p^5(^2P^\circ_{3/2})6p$	6p	[5/2]	2	9.69
$2p_8$	$5p^5(^2P^\circ_{3/2})6p$	6p		3	9.72
$2p_7$	$5p^5(^2P^\circ_{3/2})6p$	6p	[3/2]	1	9.79
$2p_6$	$5p^5(^2P^\circ_{3/2})6p$	6p		2	9.82
$2p_5$	$5p^5(^2P^\circ_{3/2})6p$	6p	[1/2]	0	9.93
$2p_4$	$5p^5(^2P^\circ_{1/2})6p$	6p′	[3/2]	1	10.96
$2p_3$	$5p^5(^2P^\circ_{1/2})6p$	6p′		2	11.05
$2p_2$	$5p^5(^2P^\circ_{1/2})6p$	6p′	[1/2]	1	11.07
$2p_1$	$5p^5(^2P^\circ_{1/2})6p$	6p′		0	11.14

https://dx.doi.org/10.1021/acs.jpclett.9b03857
J. Phys. Chem. Lett. 2020, 11, 1656−1661

symbols are similar in both cases. The ground state of xenon is of even parity. The overall parities of the excited states corresponding to $5p^5(^2P_{3/2})6s$ ($6s[3/2]^\circ_{2,1}$) and $5p^5(^2P_{1/2})6s$ ($6s'[1/2]^\circ_{0,1}$) electronic configurations are odd, which dictates that both transitions should be 1PA allowed and 2PA inactive [the superscript (°) indicates the overall odd parity of the excited state wave function (Table 1)]. The presence of the $^1S_0 \rightarrow 5p^5(^2P_{3/2})6s$ transition in the three-photon excitation of xenon further supports this parity argument, as 1PA and 3PA excitations follow similar selection rules.[46] This means that the transition to the $5p^5(^2P_{3/2})6s$ ($6s[3/2]^\circ_{2,1}$) or $5p^5(^2P_{1/2})6s$ ($6s'[1/2]^\circ_{0,1}$) state is not responsible for the band centered at ∼6.5 eV in the 2PA spectrum of aqueous iodide. However, excited states corresponding to the $5p^5(^2P_{3/2})6p$ electronic configurations are of even parity, and hence, transitions to these states (particularly the $J = 2$ and $J = 0$ subcomponents) from the ground state are 2PA parity allowed. Moore's compilation further suggests that $5p^5(^2P_{3/2})6p$ levels start ∼100 cm^{-1} above the transition to $5p^5(^2P_{1/2})6s$ (Table 1[45] and Figure 2[47]). On the basis of the excited state energies of xenon, we expect the lowest-energy two-photon allowed transition [$^1S_0 \rightarrow 5p^5(^2P_{3/2})6p$] to be centered ∼0.12−0.25 eV above the upper CTTS transition in 1PA originating from the $^1S_0 \rightarrow 5p^5(^2P_{1/2})6s$ excitation. This is consistent with our measured 2PA spectrum, which peaks ∼0.14 eV higher in energy, as compared to the upper component of the 1PA spectra,[9] shown in Figure 2c. It is worth pointing out that the literature 1PA spectrum of aqueous potassium iodide used for this comparison is measured at a high pressure (250 bar). Changing the pressure from 250 to 1 bar has only a small effect on the iodide 1PA transition energies (∼20 meV redshift),[48] and the peak positions for the CTTS transitions are the same for aqueous sodium and potassium iodide.[49] The 2PA bandwidth also appears to be different from that of the two 1PA transitions, implying different excited state character. The combined evidence thus suggests that the lowest-energy band in the 2PA spectrum of aqueous iodide is due to the $^1S_0 \rightarrow 5p^5(^2P_{3/2})6p$ transition and is unrelated to either peak observed in the 1PA spectrum. Our assignment of the 1PA and 2PA transitions in aqueous iodide is consistent with the calculated cross sections for multiphoton ionization of the isoelectronic xenon atom in the *jl* coupling limit.[50]

In ESFG spectra, under the two-photon ($\omega_1 + \omega_2$) resonant one-photon off-resonant condition (Figure 1b; ω_1 = 295 nm, blue), the intensity is proportional to the product of the 1PA and 2PA absorption cross sections at ω_{SFG} (eq 1).[30,31] It has been established above that for bulk iodide, both $^1S_0 \rightarrow 5p^5(^2P_{1/2})6s$ and $^1S_0 \rightarrow 5p^5(^2P_{3/2})6s$ transitions are 1PA allowed and 2PA forbidden, respectively, and the $^1S_0 \rightarrow 5p^5(^2P_{3/2})6p$ transition is only 2PA allowed; i.e., no electronic transition is simultaneously 1PA and 2PA active. Thus, no ESFG intensity should be observed for iodide unless the symmetry is perturbed at the interface.

There is an instantaneous asymmetry to the local solvation environment in bulk,[21] but upon moving to the interface, iodide is expected to lose approximately one or two water molecules from its first solvation shell and thus experiences far greater asymmetry.[23,51−53] In addition, at the high salt concentrations used in the ESFG experiments ($[NaI]_{bulk}$ = 5 M), solvent-shared and contact ion pairs, solvent orientational effects, and electric double-layer formation are expected.[54−56] The external electric field experienced by the iodide ion at the interface strongly perturbs the symmetry and relaxes the 1PA and 2PA parity selection rules established for bulk aqueous iodide.

When strictly resonant at only the sum frequency wavelength, ESFG intensity is observed at the interface only for the upper energy band (Figure 1b, blue). Here, the external electric field effects at the air/water interface are predicted to be more strongly affecting the upper excited states with p-like symmetry than the lower s-like excited states, allowing sufficient mixing of the 1PA and 2PA allowed transitions in the higher-energy band, and resulting in an ESFG-allowed transition. In addition, solute-solvent vibronic coupling may also enhance mixing between excited states that are energetically near-degenerate. A molecular dynamics simulation of the water molecules in the first solvation shell of the iodide ion predicts fast relaxation dynamics (∼100 fs) corresponding to the intermolecular vibrations of the ion-water hydrogen bonds.[57] Such vibronic interactions occur within the time scale of our ultrafast laser pulse durations and potentially contribute to the perturbation of the symmetry of the excited states.

We, to the best of our knowledge, are the first to report the broadband 2PA spectra of aqueous iodide and to combine ESFG with 2PA spectroscopy, where the bulk-sensitive 2PA spectra provide crucial information that aids in the interpretation of the surface-sensitive ESFG spectra. By analyzing the subtle difference in band positions in the 1PA and 2PA spectra, and considering the selection rules for these two complementary spectroscopic techniques, we show that both the $^1S_0 \rightarrow 5p^5(^2P_{3/2})6s$ and the $^1S_0 \rightarrow 5p^5(^2P_{1/2})6s$ transitions of bulk aqueous iodide that are allowed in 1PA are inactive in the 2PA counterpart. The 2PA band is assigned to the $^1S_0 \rightarrow 5p^5(^2P_{3/2})6p$ transition. It is quite unprecedented that the electronic spectra measured in a highly condensed environment can be accurately explained using the atomic selection rule for an isolated molecule, signifying that the symmetry of the lower-lying excited orbitals of "s" and "p" character are not perturbed to a great extent in the bulk liquid phase. The observed signal in the DUV-ESFG spectra must originate from symmetry breaking and solute-solvent vibronic coupling effects at the air/water interface. Further experiments and associated theoretical modeling will be necessary to extract additional details regarding these complex transitions observed in 1PA, 2PA, and ESFG spectra.

■ ASSOCIATED CONTENT

Supporting Information

The Supporting Information is available free of charge at https://pubs.acs.org/doi/10.1021/acs.jpclett.9b03857.

1PA spectra of aqueous iodide showing the literature deconvolution of the overall absorption spectrum into individual CTTS bands (PDF)

■ AUTHOR INFORMATION

Corresponding Authors

Richard J. Saykally − *Department of Chemistry, University of California, Berkeley, California 94720, United States; Chemical Sciences Division, Lawrence Berkeley National Laboratory, Berkeley, California 94720, United States;* orcid.org/0000-0001-8942-3656; Email: saykally@berkeley.edu

Stephen E. Bradforth − *Department of Chemistry, University of Southern California, Los Angeles, California 90089, United*

https://dx.doi.org/10.1021/acs.jpclett.9b03857
J. Phys. Chem. Lett. 2020, 11, 1656−1661

States; orcid.org/0000-0002-6164-3347;
Email: stephen.bradforth@usc.edu

Authors

Dhritiman Bhattacharyya − *Department of Chemistry, University of Southern California, Los Angeles, California 90089, United States;* orcid.org/0000-0001-6761-8655

Hikaru Mizuno − *Department of Chemistry, University of California, Berkeley, California 94720, United States; Chemical Sciences Division, Lawrence Berkeley National Laboratory, Berkeley, California 94720, United States;* orcid.org/0000-0002-0860-1404

Anthony M. Rizzuto − *Department of Chemistry, University of California, Berkeley, California 94720, United States; Chemical Sciences Division, Lawrence Berkeley National Laboratory, Berkeley, California 94720, United States;* orcid.org/0000-0002-1430-4414

Yuyuan Zhang − *Department of Chemistry, University of Southern California, Los Angeles, California 90089, United States*

Complete contact information is available at: https://pubs.acs.org/10.1021/acs.jpclett.9b03857

Author Contributions

‖D.B. and H.M. contributed equally to this work.

Notes

The authors declare no competing financial interest.

■ ACKNOWLEDGMENTS

The work at the University of Southern California was supported by the National Science Foundation (experimental work under Grant CHE-0617060 with assignment and analysis under Grant CHE-1665532); the work at the University of California was supported by the Director, Office of Basic Energy Sciences, Office of Science, U.S. Department of Energy, under Contract DE-AC02-05CH11231 through the Chemical Sciences Division of the Lawrence Berkeley National Laboratory. The authors thank Dr. Georg Menzl (Chemical Sciences Division, Lawrence Berkeley National Laboratory) for providing the TOC and abstract graphic.[58]

■ REFERENCES

(1) Blandamer, M. J.; Fox, M. F. Theory and Applications of Charge-Transfer-To-Solvent Spectra. *Chem. Rev.* **1970**, *70*, 59−93.
(2) Rabinowitch, E. Electron Transfer Spectra and Their Photochemical Effects. *Rev. Mod. Phys.* **1942**, *14*, 112−131.
(3) Smith, M.; Symons, M. C. R. SOLVATION SPECTRA Part 1.—The Effect of Environmental Changes upon the Ultra-Violet Absorption of Solvated Iodide Ions. *Trans. Faraday Soc.* **1958**, *54*, 338−345.
(4) Meyerstein, D.; Treinin, A. The Relation Between Lyotropic and Spectroscopic Properties of Anions in Solution. *J. Phys. Chem.* **1962**, *66*, 446−450.
(5) Stein, G.; Treinin, A. Electron-Transfer Spectra of Anions in Solution. Part 2. Temperature Dependence of Electron-Transfer Spectra of Anions in Aqueous Solution. *Trans. Faraday Soc.* **1959**, *55*, 1091−1099.
(6) Burak, I.; Treinin, A. Solvent Scale for Charge-Transfer-to-Solvent Spectra of Anions. *Trans. Faraday Soc.* **1963**, *59*, 1490.
(7) Symons, M. C. R.; Jackson, S. E. Solvation Spectra Part 60. - Specific Solvation of Iodide Ions. *J. Chem. Soc., Faraday Trans. 1* **1979**, *75* (75), 1919−1928.
(8) Blandamer, M. J.; Burdett, T. R. Effect of Pressure on the Ultra-Violet Absorption Spectra of Iodide in Non-Aqueous Solvents. *J. Chem. Soc., Faraday Trans. 2* **1972**, *68*, 577−579.
(9) Marin, T. W.; Janik, I.; Bartels, D. M. Ultraviolet Charge-Transfer-to-Solvent Spectroscopy of Halide and Hydroxide Ions in Subcritical and Supercritical Water. *Phys. Chem. Chem. Phys.* **2019**, *21*, 24419.
(10) Chen, X.; Bradforth, S. E. The Ultrafast Dynamics of Photodetachment. *Annu. Rev. Phys. Chem.* **2008**, *59*, 203−231.
(11) Matheson, M. S.; Mulac, W. A.; Rabani, J. Formation of the Hydrated Electron in the Flash Photolysis of Aqueous Solutions. *J. Phys. Chem.* **1963**, *67*, 2613−2617.
(12) Jortner, J.; Raz, B.; Stein, G. The Far u.-v. Absorption Spectrum of the Iodide Ion in Aqueous Solution. *Trans. Faraday Soc.* **1960**, *56*, 1273.
(13) Fox, M. F.; Hayon, E. Far Ultraviolet Solution Spectroscopy of the Iodide Ion. *J. Chem. Soc., Faraday Trans. 1* **1977**, *73*, 1003−1016.
(14) Fox, M. F.; Hayon, E. New CTTS Absoprtion Bands of Iodide in the Far-Ultraviolet Region. *Chem. Phys. Lett.* **1972**, *14*, 442−444.
(15) Barker, B. E.; Fox, M. F.; Walton, A. Resolution of the Far Ultraviolet Absorption Bands of Solvated Iodide. *J. Chem. Soc., Faraday Trans. 1* **1976**, *72*, 344.
(16) Kloepfer, J. A.; Vilchiz, V. H.; Lenchenkov, V. A.; Germaine, A. C.; Bradforth, S. E. The Ejection Distribution of Solvated Electrons Generated by the One-Photon Photodetachment of Aqueous I^- and Two-Photon Ionization of the Solvent. *J. Chem. Phys.* **2000**, *113*, 6288−6307.
(17) Vilchiz, V. H.; Kloepfer, J. A.; Germaine, A. C.; Lenchenkov, V. A.; Bradforth, S. E. Map for the Relaxation Dynamics of Hot Photoelectrons Injected into Liquid Water via Anion Threshold Photodetachment and above Threshold Solvent Ionization. *J. Phys. Chem. A* **2001**, *105*, 1711−1723.
(18) Sheu, W. S.; Rossky, P. J. The Electronic Dynamics of Photoexcited Aqueous Iodide. *Chem. Phys. Lett.* **1993**, *202*, 186−190.
(19) Sheu, W. S.; Rossky, P. J. Electronic and Solvent Relaxation Dynamics of a Photoexcited Aqueous Halide. *J. Phys. Chem.* **1996**, *100*, 1295−1302.
(20) Moskun, A. C.; Bradforth, S. E.; Thøgersen, J.; Keiding, S. Absence of a Signature of Aqueous $I(^2P_{1/2})$ after 200-nm Photodetachment of I^- (aq). *J. Phys. Chem. A* **2006**, *110*, 10947−10955.
(21) Bradforth, S. E.; Jungwirth, P. Excited States of Iodide Anions in Water: A Comparison of the Electronic Structure in Clusters and in Bulk Solution. *J. Phys. Chem. A* **2002**, *106*, 1286−1298.
(22) Barthel, E. R.; Martini, I. B.; Schwartz, B. J. How Does the Solvent Control Electron Transfer? Experimental and Theoretical Studies of the Simplest Charge Transfer Reaction. *J. Phys. Chem. B* **2001**, *105*, 12230−12241.
(23) Nowakowski, P. J.; Woods, D. A.; Verlet, J. R. R. Charge Transfer to Solvent Dynamics at the Ambient Water/Air Interface. *J. Phys. Chem. Lett.* **2016**, *7*, 4079−4085.
(24) Sagar, D. M.; Bain, C. D.; Verlet, J. R. R. Hydrated Electrons at the Water/Air Interface. *J. Am. Chem. Soc.* **2010**, *132*, 6917−6919.
(25) Sheu, W. S.; Rossky, P. J. Charge-Transfer-to-Solvent Spectra of an Aqueous Halide Revisited via Computer Simulation. *J. Am. Chem. Soc.* **1993**, *115*, 7729−7735.
(26) Elles, C. G.; Rivera, C. A.; Zhang, Y.; Pieniazek, P. A.; Bradforth, S. E. Electronic Structure of Liquid Water from Polarization-Dependent Two-Photon Absorption Spectroscopy. *J. Chem. Phys.* **2009**, *130* (8), 084501.
(27) Shen, Y. R. *Fundamentals of Sum-Frequency Spectroscopy*; Cambridge University Press: Cambridge, U.K., 2016.
(28) Boyd, R. W. *Nonlinear Optics*; Academic Press, 2008.
(29) Sokhan, V. P.; Tildesley, D. J. The Free Surface of Water: Molecular Orientation, Surface Potential and Nonlinear Susceptibility. *Mol. Phys.* **1997**, *92*, 625−640.
(30) Moad, A. J.; Simpson, G. J. A Unified Treatment of Selection Rules and Symmetry Relations for Sum-Frequency and Second Harmonic Spectroscopies. *J. Phys. Chem. B* **2004**, *108*, 3548−3562.

(31) Lin, C.-K.; Hayashi, M.; Lin, S. H. Theoretical Formulation and Simulation of Electronic Sum-Frequency Generation Spectroscopy. *J. Phys. Chem. C* **2013**, *117*, 23797−23805.
(32) Petersen, P. B.; Saykally, R. J. On the Nature of Ions At the Liquid Water Surface. *Annu. Rev. Phys. Chem.* **2006**, *57*, 333−364.
(33) Petersen, P. B.; Johnson, J. C.; Knutsen, K. P.; Saykally, R. J. Direct Experimental Validation of the Jones-Ray Effect. *Chem. Phys. Lett.* **2004**, *397*, 46−50.
(34) Rizzuto, A. M.; Irgen-Gioro, S.; Eftekhari-Bafrooei, A.; Saykally, R. J. Broadband Deep UV Spectra of Interfacial Aqueous Iodide. *J. Phys. Chem. Lett.* **2016**, *7* (19), 3882−3885.
(35) Mizuno, H.; Rizzuto, A. M.; Saykally, R. J. Charge-Transfer-to-Solvent Spectrum of Thiocyanate at the Air/Water Interface Measured by Broadband Deep Ultraviolet Electronic Sum Frequency Generation Spectroscopy. *J. Phys. Chem. Lett.* **2018**, *9*, 4753−4757.
(36) Kothe, A.; Wilke, M.; Moguilevski, A.; Engel, N.; Winter, B.; Kiyan, I. Y.; Aziz, E. F. Charge Transfer to Solvent Dynamics in Iodide Aqueous Solution Studied at Ionization Threshold. *Phys. Chem. Chem. Phys.* **2015**, *17*, 1918−1924.
(37) Messina, F.; Bräm, O.; Cannizzo, A.; Chergui, M. Real-Time Observation of the Charge Transfer to Solvent Dynamics. *Nat. Commun.* **2013**, *4*, 2119.
(38) Tauber, M. J.; Mathies, R. A.; Chen, X.; Bradforth, S. E. Flowing Liquid Sample Jet for Resonance Raman and Ultrafast Optical Spectroscopy. *Rev. Sci. Instrum.* **2003**, *74*, 4958−4960.
(39) Bhattacharyya, D.; Zhang, Y. G.; Elles, C. E.; Bradforth, S. Electronic Structure of Liquid Methanol and Ethanol from Polarization-Dependent Two-Photon Absorption Spectroscopy. *J. Phys. Chem. A* **2019**, *123*, 5789−5804.
(40) Franck, J.; Scheibe, G. Über Absorptionsspektren Negativer Halogenionen in Lösung. *Z. Phys. Chem.* **1928**, *139A*, 22 DOI: 10.1515/zpch-1928-13904.
(41) Jortner, J.; Ottolenghi, M.; Stein, G. On the Photochemistry of Aqueous Solutions of Chloride, Bromide, and Iodide Ions. *J. Phys. Chem.* **1964**, *68*, 247−255.
(42) Platzman, R.; Franck, J. The Role of the Hydration Configuration in Electronic Processes Involving Ions in Aqueous Solution. *Eur. Phys. J. A* **1954**, *138*, 411−431.
(43) Jortner, J.; Treinin, A. Intensities of the Absorption Bands of Halide Ions in Solution. *Trans. Faraday Soc.* **1962**, *58*, 1503−1510.
(44) Herzberg, G. *Atomic Spectra and Atomic Structure*, 2nd ed.; Dover Publications: New York, 1944.
(45) Moore, C. E. *Atomic Energy Levels as Derived from the Analysis of Optical Spectra*; National Bureau of Standards: Washington, DC, 1952; Vol. *2*.
(46) Faisal, F. H. M.; Wallenstein, R.; Zacharias, H. Three-Photon Excitation of Xenon and Carbon Monoxide. *Phys. Rev. Lett.* **1977**, *39*, 1138−1141.
(47) Ku, J. K.; Setser, D. W. Collisional Deactivation of Xe($5p^5 6p$) States in Xe and Ar. *J. Chem. Phys.* **1986**, *84*, 4304−4316.
(48) Blandamer, M.; Gough, T.; Symons, M. C. R. Solvation Spectra. Part 5.—Effect of Pressure on the Ultra-Violet Absorption Spectrum of Solvated Iodide. *Trans. Faraday Soc.* **1963**, *59*, 1748−1753.
(49) Griffiths, T. R.; Wijayanayake, R. H. Effects of Cations upon Absorption Spectra Part 5.-Charge-Transfer-to-Solvent Spectrum of Iodide and Ion-Pair Formation. *Trans. Faraday Soc.* **1970**, *66*, 1563−1573.
(50) McGuire, E. J. Two- and Three-Photon Ionization in the Noble Gases. *Phys. Rev. A: At., Mol., Opt. Phys.* **1981**, *24*, 835−848.
(51) Otten, D. E.; Shaffer, P. R.; Geissler, P. L.; Saykally, R. J. Elucidating the Mechanism of Selective Ion Adsorption to the Liquid Water Surface. *Proc. Natl. Acad. Sci. U. S. A.* **2012**, *109*, 701−705.
(52) Stern, A. C.; Baer, M. D.; Mundy, C. J.; Tobias, D. J. Thermodynamics of Iodide Adsorption at the Instantaneous Air-Water Interface. *J. Chem. Phys.* **2013**, *138*, 114709.
(53) Caleman, C.; Hub, J. S.; van Maaren, P. J.; van der Spoel, D. Atomistic Simulation of Ion Solvation in Water Explains Surface Preference of Halides. *Proc. Natl. Acad. Sci. U. S. A.* **2011**, *108*, 6838−6842.
(54) Venkateshwaran, V.; Vembanur, S.; Garde, S. Water-Mediated Ion-Ion Interactions Are Enhanced at the Water Vapor-Liquid Interface. *Proc. Natl. Acad. Sci. U. S. A.* **2014**, *111*, 8729−8734.
(55) Ishiyama, T.; Morita, A. Intermolecular Correlation Effect in Sum Frequency Generation Spectroscopy of Electrolyte Aqueous Solution. *Chem. Phys. Lett.* **2006**, *431*, 78−82.
(56) Ishiyama, T.; Morita, A. Molecular Dynamics Study of Gas-Liquid Aqueous Sodium Halide Interfaces. I. Flexible and Polarizable Molecular Modeling and Interfacial Properties. *J. Phys. Chem. C* **2007**, *111*, 721−737.
(57) Karmakar, A.; Chandra, A. Water in Hydration Shell of an Iodide Ion: Structure and Dynamics of Solute-Water Hydrogen Bonds and Vibrational Spectral Diffusion from First-Principles Simulations. *J. Phys. Chem. B* **2015**, *119*, 8561−8572.
(58) Humphrey, W.; Dalke, A.; Schulten, K. VMD: Visual Molecular Dynamics. *J. Mol. Graphics* **1996**, *14*, 33−38.

https://dx.doi.org/10.1021/acs.jpclett.9b03857
J. Phys. Chem. Lett. 2020, 11, 1656−1661